


Research article

Hygrothermal Performance of Roofs with High Initial Construction Moisture Subjected to Hot Climate

Hamed H. Saber¹ ^a

¹ Jubail Industrial College and Deanship of Research and Industrial Development, Royal Commission of Jubail and Yanbu, Jubail Industrial City 31961, Saudi Arabia

Keywords: Moisture performance, energy performance, cool roof, black roof, mould growth

<https://doi.org/10.53370/001c.118788>

Yanbu Journal of Engineering and Science

Vol. 21, Issue 1, 2024

Abstract

Moisture accumulation in the building components/assemblies that form building envelopes can lead to material deterioration and moisture related issues such as mould growth. As a part of the building envelope, this study focusses on assessing the moisture performance and energy performance (i.e., hygrothermal performance) of roofing systems. As roofs can be built with high initial construction moisture, numerical simulations were conducted with and without high initial construction moisture in order to investigate: (a) the hygrothermal performance of cool and black roofs having material layer with high initial construction moisture content, (b) the time needed so that the moisture content reaches acceptable level as per the building code requirements, (c) whether moisture accumulation and mould growth occur in the roofs, and (d) the energy savings as a result of installing white/cool roof instead of black roof. An advanced numerical model is used to conduct the numerical simulations for black and cool roofs when they are subjected to hot climate. This model solves simultaneously the Heat, Air and Moisture (HAM) transport equations in all layers of the building assemblies. The model was extensively validated by comparing its predictions with the experimental data of different building components at various operating conditions. For the roofing systems investigated in this paper, the results showed that mould growth occurred in the black and cool roofs only for the case with high initial construction moisture. The mould has totally disappeared after 378.8 day for the black roof and 479.3 day for the cool roof. The temperatures of the cool roof were much lower than those for the black roof. The total yearly energy load with the black roof was 77% greater than that with the cool roof.

INTRODUCTION

The phenomenon of global warming is one of the problems that we currently face. This phenomenon has led to many environmental issues including higher atmospheric temperatures, increased intensity of precipitation, and increased greenhouse gas emissions.¹ Due to sharp increase in the energy demands, buildings and other built environments have a significant role in contributing to the global consequences of climate change. In regions with harsh climatic conditions, a substantial share of energy is used for heating and cooling the buildings.² Improving the thermal performance of building envelope components³⁻⁶ as well as the thermal performance of the mechanical systems (e.g., heat exchangers, ducts, etc.⁷⁻⁹) would result in reducing the energy demand and thus contributing to the fight against

global warming. Several studies have shown the potential benefits of green and cool roofs in terms of energy conservation, lowering urban heat islands, reducing global warming via decreased greenhouse gas emissions, and as well minimizing the local air pollution.^{5,6,9-13}

The implementation of roofs that possess high energy performance and exhibit little susceptibility to moisture-related issues can effectively contribute to the reduction of energy consumption in building.¹⁰⁻¹³ Green roofs are widely used due to its lightweight, thin growing media, limited or no maintenance, low cost, and high potential application for use in the new or existing lightweight structures. As provided in,¹² green roof was able to reduce the heat gain by 66% during the cooling months. Bentz¹³ provided a realistic method for choosing and designing a green reroofing system. Both thermal insulation properties and solar reflectivity of the roof surface have significant effect on the

a Email: saberh@rcjy.edu.sa

roof performance. Tariku et al.⁵ conducted a review on the impact of temperature, moisture, and aging on the in-service performance of commonly used insulation materials for flat roofs. That study provided mathematical expressions for the thermal conductivity as a function of temperature and moisture content that can be used for assessing the long-term energy and moisture performance of roofing systems. As the thermal conductivity and heat capacity are among the most essential properties of a building insulation, ignoring the temperature dependency of these material properties may lead to under and over estimations of buildings energy uses and the corresponding equipment sizing.⁴

The influence of roof solar reflectivity (α_s) on the cooling and heating loads for buildings in the US was investigated by Akbari et al.¹⁴ The findings of simulations conducted on a one-story house demonstrated that enhancing α_s from 20% to 60% is equivalent in value to more than half of the insulation in the roof subjected to hot climates.¹⁵ For a single-story building in Boston having a roof with thermal resistance (R-value) of 2.7 m²·K/W, a 13% reduction in energy consumption was achieved by doubling the existing insulation; whereas installing a green roof instead of this roof resulted in a 12% reduction in energy use.¹⁶

Roof experiences drying due to the absorbed solar radiation during daylight hours. The selections of the exterior coating and membrane for the cool roof are influenced by the major property of α_s .¹⁷⁻²¹ Therefore, it is important to design roof toward achieving energy savings while minimizing the potential for moisture-related issues. The findings from the simulation results for black and cool roofs indicated that cool roofs exhibited higher level of stored moisture in the winter compared to black roofs.^{22,23} As well, Saber et al.¹⁸ showed that the utilization of cool roofs in the climates of Saskatoon (SK) and St. John's (NL) have resulted in enduring issues associated to moisture accumulation. The initial construction moisture in roof may have impact on the energy performance and the sustainability. With initial construction moisture, Bludau et al.²⁴ showed that cool roofs exhibited significantly lower temperatures and a reduced capacity for drying compared to black roofs.

During the construction phase, roofs can be built with high initial construction moisture. On the other hand, conducting numerical simulation to assess the hygrothermal performance of a building assembly (roof in this study) requires knowing the initial conditions of temperature, moisture content and velocity in all building layers that are needed to solve the Heat, Air and Moisture (HAM) equations. In most of cases, these initial conditions are unknown. Consequently, values for these initial conditions are assumed in order to perform the numerical simulations. To the best of the author knowledge, no such study is available to investigate the long-term hygrothermal performance of black and cool roofs with high initial construction moisture in order to determine: (a) the time period needed so that moisture content in the roofs reaches an acceptable level by the building code authorities, (b) whether or not mould growth occurs during the time period in which the moisture content in the roof is greater than the acceptable value,

and (c) the time beyond which the effect of using initial conditions has no effect on the hygrothermal performance of the roofs. Thus, for Modified-Bitumen (MOD-BIT) roofs, the objectives of this study are to: (a) assess the moisture performance of black and cool roofs in case of using roof layer (Fibreboard in this study, see [Figure 1](#)) with high initial construction moisture content, (b) identify the period needed so that the moisture content would reach an acceptable limit by the building codes, for example, the National Building Code of Canada,²⁵ and (c) determine the time beyond which the energy performance and moisture performance are totally independent on the initial conditions.

INTERACTION BETWEEN HEAT, AIR AND MOISTURE IN BUILDING ENVELOPE

Assessing the performance of a building envelope component (e.g., wall, roof, windows, curtain wall, and skylight device) requires: (a) conducting field and/or laboratory tests, and/or (b) conducting numerical simulations with validated numerical models. Heat, air and moisture transports occur in the building component/assembly as a result of subjecting it to various environmental conditions for the indoor and the outdoor.²⁶⁻³⁰ In other words, heat transport, air transport and moisture transport, respectively, through a building assembly, occur due to temperature gradient, vapor pressure gradient, and air pressure difference across the assembly. With heat transport at different indoor and outdoor conditions, several previous studies have shown that the air transport in building assemblies due to natural convections and air leakage thorough the assembly at various pressure differences can result in significant reductions in the R-values of the assemblies (e.g., see²⁷⁻³²). In addition, moisture transport phenomena and its related issue such as mould growth or mould decay are much slower processes in relation to the other phenomena related to heat and air transports. Therefore, the time period that is needed to assess the hygrothermal performance of a building assembly could be long (e.g., sometimes period of order of years as presented in this study).

The obtained performance of a building assembly from tests or numerical simulations is specific to the environmental conditions in which the assembly is subjected to. For other environmental conditions, assessing the performance may require repeating the tests or the numerical simulations at these conditions. In many cases, conducting field or laboratory tests are time consuming and costly. On the other hand, assessing a long-term performance may require conducting the tests during long periods, resulting in more time consuming and more cost. However, validating a numerical model against the test data and then use it to assess the performance of building assemblies subjected to different environmental conditions (i.e., different indoor conditions and different climatic conditions) could lead to less time consuming and less cost.

The hygrothermal properties of a construction material (e.g., thermal conductivity, specific heat, water vapor permeability, etc.) depend on the local temperature and moisture content distributions inside the material layers. Additionally, both water vapor permeance and liquid diffusivity

of construction materials are important properties that have direct effect on the moisture transport through the building assemblies. In the design phase of buildings (e.g., THE LINE, hospitals, etc.), the selection of the types of construction materials should be taken into consideration in order to minimize the risk of condensation and its related issues such as mould growth and indoor air quality. For example, the performance of a building assembly at a dry condition could be different from that for the same assembly at a wet condition (see²⁻⁴ for more details). This is because the thermal conductivity (as example) of a dry material is less than that at wet condition. As such, hygrothermal models should solve the coupled partial differential equations for heat transport, moisture transport and air transport, and simultaneously accounting for the dependencies of the hygrothermal properties on both temperature and moisture content. In this paper, a validated numerical model against field and laboratory test data is used to assess the long-term energy and moisture performance of the roofing systems (Figure 1), subjected to natural climatic conditions. This model is described next.

MODEL DESCRIPTIONS AND VALIDATIONS

For assessing the energy and moisture performance of various components of building envelopes, the previously developed model²⁶⁻³⁰ that is used in this study solves simultaneously: (a) the energy equation, (b) the moisture transport equation, (c) the air transport equation, (d) the surface-to-surface radiation equation, and (e) the surface-to-ambient radiation equation. In this study, the surface-to-surface radiation equation is needed to account for the heat transfer by radiation on all surfaces that bound the enclosed-airspace shown in green in Figure 1. Also, the surface-to-ambient radiation equation is needed to account for solar radiation and thermal radiative exchange between the roof exterior surface, sky, and environment, where the environment includes the ground and adjacent constructions/buildings.

For porous material layers (all layers in the roof shown in Figure 1 except the steel deck and the enclosed airspace), the air transport equation is the Darcy equation for Darcy number (D_N) less than 10^{-6} and Brinkman equation for Darcy number greater than 10^{-6} . For the air layers (e.g., the enclosed-airspace between the steel deck and the vapor membrane) the air transport equation is the compressible momentum equation (Navier-Stoke equation). The full descriptions of the governing equations mentioned above are not repeated in this paper as they are available in.²⁶⁻³⁰ These equations were discretized using the finite element method (FEM). The use of the FEM is important as it permits meshing complicated geometries with less discretizing errors. Due to symmetry, numerical simulations were conducted for the computational domain shown in Figure 1c, where sensitivity analyses were conducted for determining the numerical mesh size. Figure 5 shows the mesh distribution in the roofing system that has resulted in a mesh independent solution in which the total number of triangular elements is 16067, which includes: (a) 1012 elements

in the applied asphalt based membrane, (b) 1302 elements in the Fiberboard, (c) 2213 elements in the polyisocyanurate board, (e) 1192 elements in felt membrane, (f) 4388 elements in the steel deck, and (g) 5960 elements in the enclosed-airspace (see Figure 1c).

The model was extensively validated against experimental data obtained from laboratory and field tests for different building components with various types of insulations including reflective insulations.²⁶⁻⁴² For walls with Insulating Concrete Form (ICF) and subjected to climatic conditions of Ottawa (ON), the model predictions were in good agreement with field data.³³ Additionally, the model was validated against field measurements for highly insulated residential wood-frame construction incorporating vacuum insulated panels, VIPs (see,³⁴⁻³⁶ for more details). The model was used to compare the predicted drying rate of four full-scale wall assemblies (Set-1, Set-2, Set-3 and Set-4) incorporating wet oriented strand board (OSB) with the test data.^{26,37,38} As shown in Figure 2, the measured average moisture content (MC) in the OSB over the test period were in good agreement with the model predictions (within $\pm 5\%$).²⁶ The predicted R-values of a number of full-scale walls called “WER” having various types of thermal insulations (WER-1 and WER-5 incorporating glass fibre batts, and WER-AA, WER-BB, WER-CC and WER-DD incorporating open-cell polyurethane spray foams) were compared with the measured R-values using Guarded Hot Box (GHB) in accordance with ASTM C1363.³⁹ Figure 3 shows that the model predictions were in good agreement with measured R-values to within $\pm 5\%$.²⁷ Also, the measured R-value using GHB in accordance with ASTM C1363³⁹ for above-grade wall system with reflective insulation ($4.24 \text{ m}^2\cdot\text{K}/\text{W}$) was in good agreement with the predicted R-value ($4.19 \text{ m}^2\cdot\text{K}/\text{W}$) being within $\pm 1.2\%$.²⁸ For small-scale building components, the test data of reflective insulation assemblies obtained using Heat Flow Meter (HFM) in accordance with the ASTM C518⁴⁰ were compared with the model predictions, where the predicted heat fluxes were in good agreement with test data to within $\pm 1.0\%$.^{41,42} With reflective insulations, most recently, the model predictions were compared with test data from the U.S. National Bureau of Standards for the R-values obtained using hot-box for horizontal single and double enclosed-airspaces with heat flow up and heat flow down, and vertical single and double enclosed-airspaces with heat flow horizontal.⁴³ As shown in Figure 4, the results showed that the model predictions for R-values of enclosed-airspaces of various conditions were in good agreement with the test data being within +4% and -7% (see^{29,30} for more details). After extensively validating the model, it is used in this study with confidence to assess the hygrothermal performance of black and cool roofs with and without high initial construction moisture content.

ROOF DESCRIPTIONS

A schematic of the roofing system “Modified-Bitumen, MOD-BIT” used in this study is shown in Figure 1. The MOD-BIT roof consists of: (a) cap sheet (3.67 mm thick) and base sheet (3.67 mm thick) made of torch applied as-

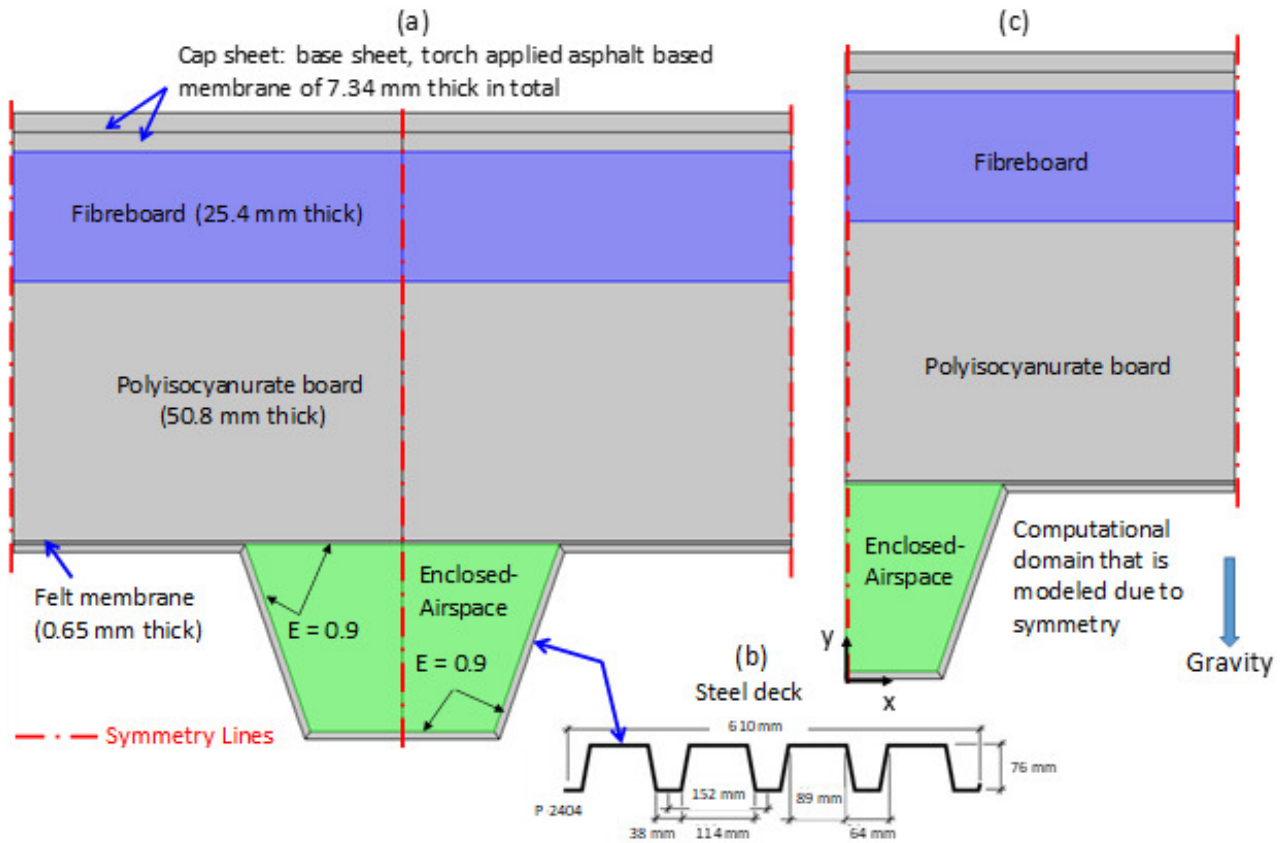


Figure 1. Modified-Bitumen (MOD-BIT) roof

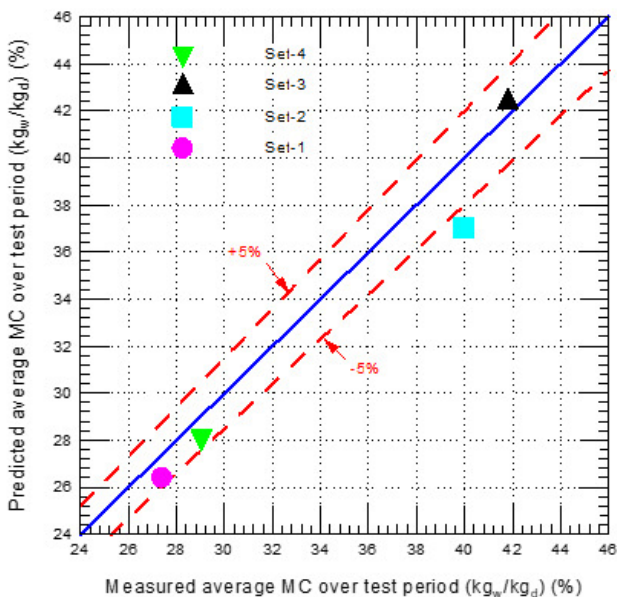


Figure 2. Comparison between the predicted and measured average moisture content in the OSB over the period of the test²⁶

phalt based membrane, (b) fibreboard (25.4 mm thick), (c) thermal insulation made of rigid polyisocyanurate board (50.8 mm thick), (d) vapour barrier made of bituminous paper (0.65 mm thick), and (e) steel deck. As per the dimen-

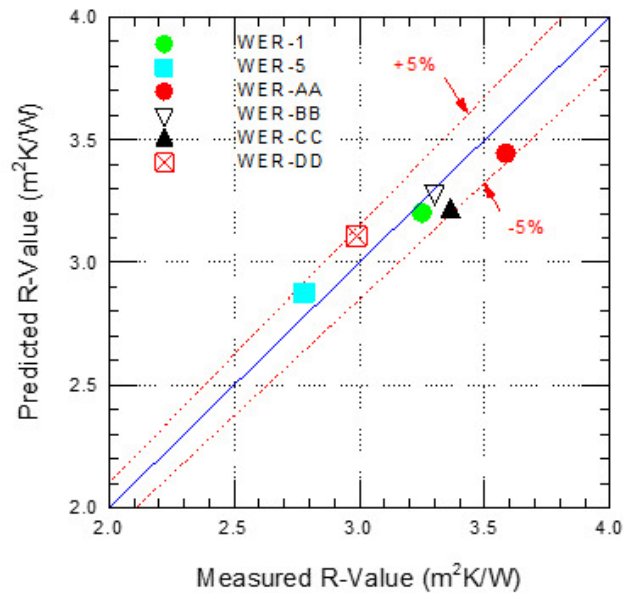


Figure 3. Comparison between the predicted and measured R-values of full-scale wall assemblies²⁷

sions provided in [Figure 1](#), the hydraulic diameter of the enclosed-airspace between the steel deck and vapour barrier is 41.3 mm. It is assumed that all material layers shown in [Figure 1](#) are in good contact. As such, the resistances to heat and moisture transfer at the interfaces of the material

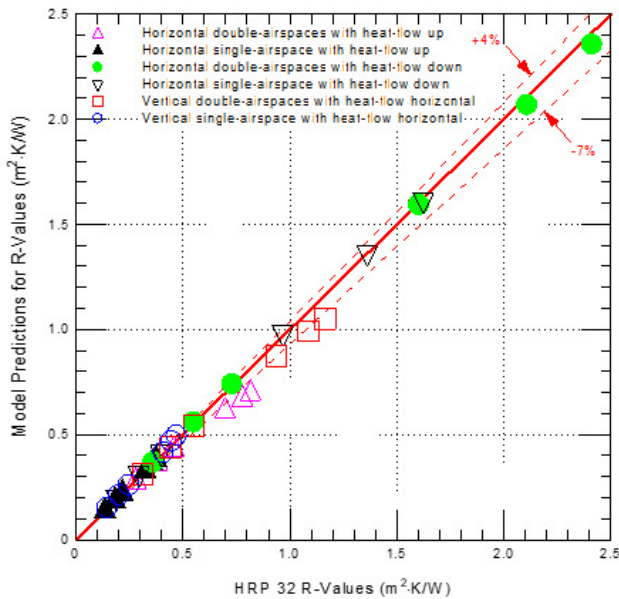


Figure 4. Comparison of model predictions for R-values with HRP 32 R-values for enclosed-airspaces with wide range of effective emittance⁵⁰

layers are neglected. However, the model has the capability to account for the effect of these interfacial resistances in case if they are known. The hygrothermal properties of the roof materials are obtained from material database provided in.⁴⁴ All surfaces that bound the enclosed-airspace between the steel deck and the vapor barrier as well as the roof exterior surface have emittance of 0.9.⁴⁵ In order to consider the presence of perforations and joints in the steel deck, a value of 3.3 m (5 US perms) was assigned to its vapour permeance.^{21,23} In this study, the short-wave solar reflectivity (α_s) for the exterior surfaces of the cool roof and black roof, respectively, are 80% and 12%.^{18,23} Note that the value of α_s can decrease with time due to ageing and/or dust accumulation.²⁴ For hot and dusty climate in Saudi Arabia, the reductions in α_s were accounted for in previous studies.⁴⁶⁻⁴⁸

BOUNDARY AND INITIAL CONDITIONS

The climate of Phoenix (AZ) was used to investigate the moisture performance of cool and black roofs with high initial construction moisture. In previous study,¹⁸ the indoor conditions based on the ASHRAE recommendations for conditioned space⁴⁹ and the European standard, EN 15026⁵⁰ were used to assess the long-term performance of black and cool roofs, subjected to several climates in North America. The results of that study showed that using the indoor conditions based on EN 15026⁵⁰ have resulted in that both black and cool roofs run with higher moisture content in relation to those using the ASHRAE indoor conditions.⁴⁹ Thus, the indoor conditions based on EN 15026⁵⁰ are used in this study. The EN 15026 indoor conditions are⁵⁰:

$$T_{ind} = \begin{cases} 20 \text{ }^\circ\text{C} & \text{for } T_{outd} \leq 10 \text{ }^\circ\text{C} \\ 0.5T_{outd} + 15 \text{ }^\circ\text{C} & \text{for } 10 \text{ }^\circ\text{C} \leq T_{outd} \leq 20 \text{ }^\circ\text{C} \text{ and} \\ 25 \text{ }^\circ\text{C} & \text{for } T_{outd} \geq 20 \text{ }^\circ\text{C} \end{cases}$$

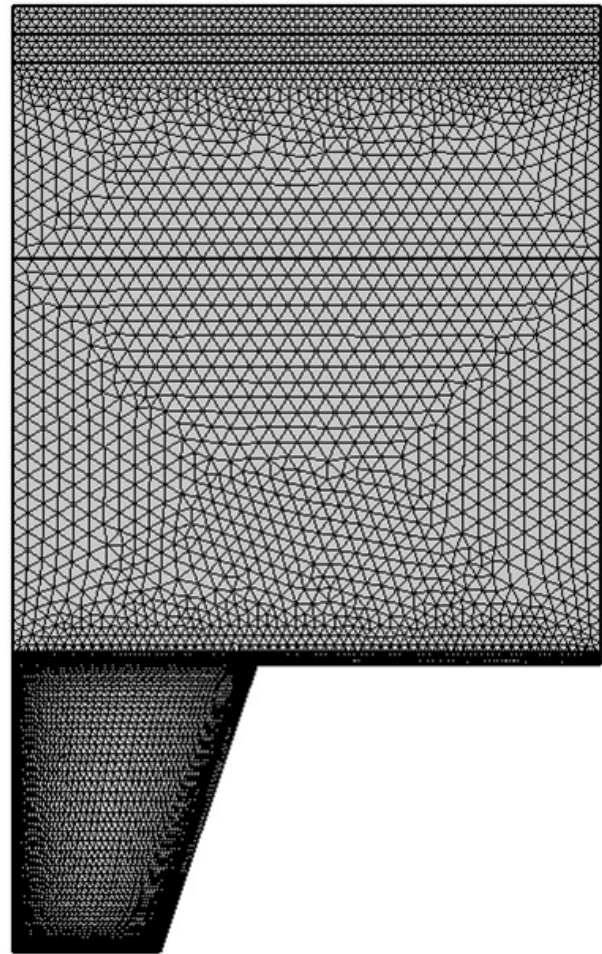


Figure 5. Numerical mesh in the MOD-BIT roof

$$RH_{ind} = \begin{cases} 30\% & \text{for } T_{outd} \leq -10 \text{ }^\circ\text{C} \\ T_{outd} + 40\% & \text{for } -10 \text{ }^\circ\text{C} \leq T_{outd} \leq 20 \text{ }^\circ\text{C} \text{ and} \\ 60\% & \text{for } T_{outd} \geq 20 \text{ }^\circ\text{C} \end{cases} \quad (1)$$

In Eq. (1), T_{ind} and T_{outd} are the indoor air temperature and the outdoor air temperature (from the weather data), respectively ($^\circ\text{C}$). Also, RH_{ind} is the indoor relative humidity (%).

Due to symmetry, the computational domain that is modeled is shown in [Figure 1c](#). The boundary conditions that are needed to solve the air transport equation are: (a) non-slip condition for the air on the surface of the steel deck, and (b) symmetry condition on the right and left boundaries. The boundary conditions needed to solve the energy equation are: (a) symmetry condition on the right and left boundaries, (b) heat flux on the outdoor surface ($q_{h,outd}$), and (c) heat flux on the indoor ($q_{h,ind}$). The surface-to-surface radiation equation is subjected to emittance of 0.9⁴⁵ for all surfaces that bound the enclosed-air-space. For the surface-to-ambient radiation equation, the emittance of the exterior surface of cool and black roof is 0.9⁴⁵; whereas the values of the short-wave solar reflectivity (α_s) are 80% and 12% for cool roof and black roof, respectively.^{23,24} For moisture transport equation, the boundary conditions needed to solve this equation are: (a) symmetry condition on the right and left boundaries, (b) moisture flux on the outdoor surface ($q_{m,outd}$), and (c)

moisture flux on the indoor system ($q_{m,ind}$). For given outdoor and indoor conditions, the detailed procedures for determining $q_{h,out}$, $q_{h,ind}$, $q_{m,out}$ and $q_{m,ind}$ are provided in.^{18,37} As well, these procedures included the evaluations of the heat transfer coefficients and mass transfer coefficients on the outdoor surface and the indoor surface that are needed for determining $q_{h,out}$, $q_{h,ind}$, $q_{m,out}$ and $q_{m,ind}$.

As the initial moisture contents in the material layers are unknown, and thus are assumed in this study, the errors coming from disregarding the capillary hysteresis are also unknown. However, as this study deals with comparisons of black roof performance with cool roof performance using the same assumptions in both roofs, the conclusions are unbiased and correct. As initial condition for air transport equation, the air velocities in x- and y-directions are set to 0.0. For the energy equation, the initial temperatures are set to 10 °C in all roof layers. For moisture transport equation, the initial moisture contents in all materials of the roofing layers except the Fibreboard are set to correspond a relative humidity (RH) of 50%. However, the Fibreboard is sensitive to moisture absorption and desorption, and mould growth in relation to the other materials in the MOD-BIT roof. To investigate the roof performance for the scenario of installing the Fibreboard with High Initial Construction Moisture (HICM) and sealing the roof before allowing it to dry, the initial relative humidity (RH) in the Fibreboard is set at 95%, which corresponds to moisture content of 36.8% kg_w/kg_{dm} . This scenario is called “Fibreboard with HICM”. For the purpose of comparisons, another scenario is considered called “Reference Case” in which the initial moisture content in the Fibreboard corresponds to 50% RH (i.e., its initial RH is same as the other material layers in the roofing system). For this Reference Case and the same types of roofing systems considered in this study (Figure 1), previous studies^{18,51} were conducted to investigate the long-term performance of black and cool roofs when they were subjected to different climates of North America with various Heating Degree Days (HDD), namely: Toronto (ON), Montreal (QC), St John’s (NL), Saskatoon (SK), Seattle (WA), Wilmington (NC), and Phoenix (AZ). The HDD for these cities are 3520, 4200, 4800, 5700, 2564, 1349, and 578, respectively. Additionally, for different types of roofing systems, other previous studies were conducted to investigate the long-term performance of black and cool roofs when they are subjected to Saudi and Kuwaiti climates.^{37,38,46-48, 52-54}

DATA REDUCTION

As the present model solves the HAM equations, the results of the numerical simulations include the local distributions in all roofing layers for the relative humidity (RH) and the corresponding moisture content (MC), temperature (T) and the corresponding heat flux, and air velocity components. In this study, derived parameters P (e.g., T, RH, MC) from the simulation results are used to assess the hygrothermal performance of the roofing systems. For a given material

layer, the volume-weighted and the area-weighted average parameter P are calculated as following:

$$P_{avg,V} = \frac{1}{V} \int_V P(t) \cdot dV, \quad (2)$$

$$\text{and } P_{avg,A} = \frac{1}{A} \int_A P(t) \cdot dA,$$

where, V is the volume of the material layer and A is the surface area at the interface between the material layers. The derived value for $P_{avg,V}$ in Eq. (2) corresponds to $T_{avg,V}$, $MC_{avg,V}$ and $RH_{avg,V}$ for the volume-weighted average temperature, moisture content and relative humidity, respectively. Also, the derived value for $P_{avg,A}$ in Eq. (2) for a given interface at the material layers corresponds to $T_{avg,A}$ and $RH_{avg,A}$ for the area-weighted average temperature and relative humidity, respectively. In addition, the values for the area-weighted moisture content ($MC_{avg,A}$) is derived from the relative humidity values through the sorption-desorption property at the interface of each material layer.

The local heat flux normal to the indoor surface of the roofing system shown in Figure 1 ($q_{ind,surf}$) is used to determine the monthly and yearly heating energy load ($E_{H,L}$), and the monthly and yearly cooling energy load ($E_{C,L}$). Note that when $q_{ind,surf}$ is positive, it is called “heat gain” (i.e., heat into the building where the roof contributes to an increased cooling load). Also, when $q_{ind,surf}$ is negative, it is called “heat loss” (i.e., heat out of the building where the roof contribute to an increased heating load). The values of $E_{H,L}$ and $E_{C,L}$ are obtained from the following numerical integrations:

$$E_{H,L} = \int_{t_1}^{t_2} \begin{pmatrix} q_{ind,surf} \text{ for } q_{ind,surf} < 0 \\ 0 \text{ for } q_{ind,surf} \geq 0 \end{pmatrix} dt, \text{ and}$$

$$E_{C,L} = \int_{t_1}^{t_2} \begin{pmatrix} q_{ind,surf} \text{ for } q_{ind,surf} > 0 \\ 0 \text{ for } q_{ind,surf} \leq 0 \end{pmatrix} dt. \quad (3)$$

For monthly energy loads, t_1 and t_2 in Eq. (3) are the times at the beginning and end of the month, respectively. Whereas, for yearly energy loads, $t_1 = 0$ and $t_2 = 365$ day.

RESULTS AND DISCUSSIONS

With the model, and the boundary and initial conditions provided earlier, this section discusses the simulation results for the long-term performance for black and cool roofs. To find out whether mould growth occurs in the roofs, both temperature (T) and relative humidity (RH) in the roof layers are the key parameters that have direct effects on mould growth.^{55,56} These parameters (T and RH) are derived from the numerical simulation results as shown in the previous section. For mould growth in construction materials, the classifications of these materials for mould growth are provided in.⁵⁷ For the roof shown Figure 1, the Fibreboard is classified as “Sensitive”; whereas polyisocyanurate board is classified as “Medium Resistant”.

MOISTURE PERFORMANCE

Two scenarios were simulated for both black and cool roofs. The first represents the case of Fibreboard with high initial construction moisture called “Fibreboard with HICM” in which the initial moisture content corresponds to 95% RH.

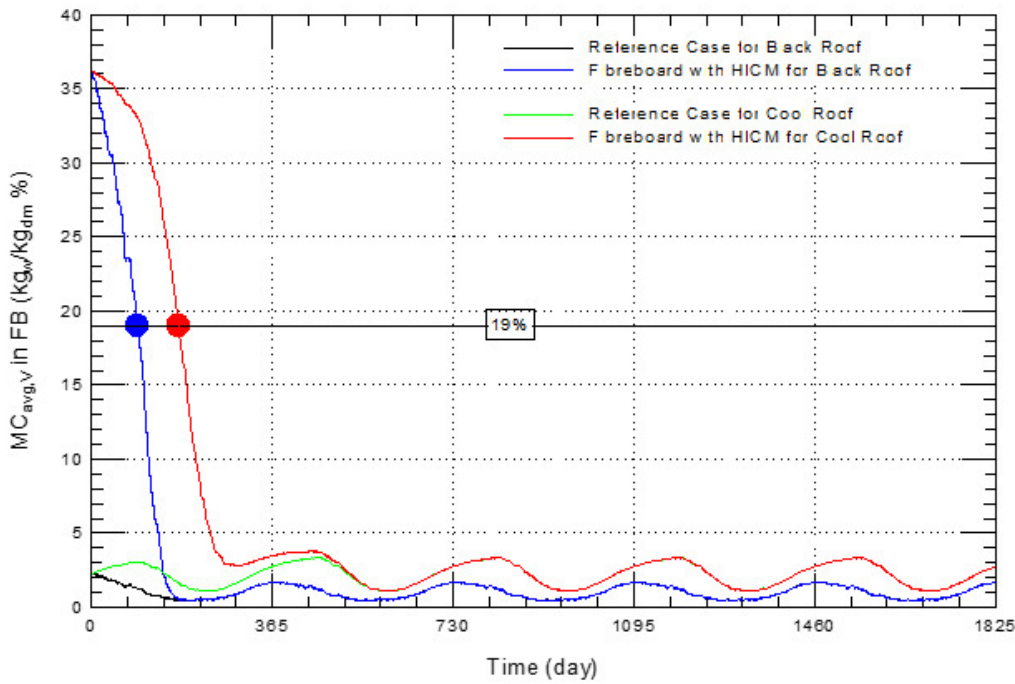


Figure 6. Volume-weighted average moisture content ($MC_{avg,V}$) in the Fibreboard

Whereas the second represents the case of dry Fibreboard called “Reference Case” in which the initial moisture content in the Fibreboard corresponds to 50% RH. To assess both the energy performance and moisture performance, all numerical simulations were conducted for a period of 5 years. In the figures of this paper, time equal to zero corresponds to January 1st. For black and cool roofs, Figure 6 shows the variation of volume-weighted average moisture content ($MC_{avg,V}$) in the Fibreboard with time for the Reference Case and Fibreboard with HICM. Also, Figure 7 shows the corresponding results for the volume-weighted average relative humidity ($RH_{avg,V}$) in the Fibreboard with time. Within the simulation period, the values of $MC_{avg,V}$ and $RH_{avg,V}$ are evaluated using Eq. (2). Some building codes requires that the moisture content in wood-based elements to be below 19% kg_w/kg_{dm} (e.g., see the National Building Code of Canada, NBCC²⁵). For the case of Fibreboard with HICM, the initial moisture content in the Fibreboard is 36.8% kg_w/kg_{dm} , which corresponds to relative humidity of 95%.

During the first year for the black roof, Figure 6 and Figure 7, respectively, show that the moisture content and the relative humidity in the Fibreboard decrease with time for both Reference Case and the Fibreboard with HICM until reaching their lowest value at 196 day. The lowest values of $MC_{avg,V}$ (0.5% kg_w/kg_{dm}) and $RH_{avg,V}$ (15.3%) are the same for both Reference Case and the Fibreboard with HICM. For the case of Fibreboard with HICM, Figure 6 shows that $MC_{avg,V}$ decreases from its initial (36.8% kg_w/kg_{dm}), and reaches its permissible limit of 19% kg_w/kg_{dm} as per the NBCC²⁵ at 92.6 day. At this time, $MC_{avg,V}$ for the Reference Case is only 1.25% kg_w/kg_{dm} . For both Reference Case and Fibreboard with HICM, $MC_{avg,V}$ and $RH_{avg,V}$ during the sec-

ond year are the same as those during the subsequent years (Figure 6 and Figure 7).

Besides showing the volume-weighted average for relative humidity in the Fibreboard (Figure 7), it is also important to show the relative humidity distribution in the other locations of the Fiberboard. For both Reference Case and Fibreboard with HICM in the black and cool roofs, Figure 8 shows the area-weighted average relative humidity ($RH_{avg,A}$) on the Fibreboard top surface (cap sheet – Fibreboard interface) and on the Fibreboard bottom surface (Fibreboard – polyisocyanurate interface). The values of the RH inside the Fibreboard, however, are within the range between the value of RH on the top surface and the value of RH on bottom surface. At the time at which $MC_{avg,V}$ for the case of Fibreboard with HICM reaches 19% kg_w/kg_{dm} (i.e., 92.6 day), the values of $RH_{avg,A}$ on the top surface and bottom surface, respectively, are 81.6% ($MC_{avg,A} = 9.6\%$ kg_w/kg_{dm}) and 93.0% ($MC_{avg,A} = 26.9\%$ kg_w/kg_{dm}) compared to only 36.6% ($MC_{avg,A} = 1.3\%$ kg_w/kg_{dm}) and 40.5% ($MC_{avg,A} = 1.5\%$ kg_w/kg_{dm}) for the Reference Case. However, the time at which the value of $MC_{avg,A}$ reaches 19% kg_w/kg_{dm} on the top surface is 86.2 day, which is shorter than that on the bottom surface (109.7 day).

Regarding the case of Fibreboard with HICM in cool roof, Figure 6 shows that $MC_{avg,V}$ reaches the threshold value of 19% kg_w/kg_{dm} at 175.7 day, which is about twice that for black roof (92.6 day). For the time at the threshold value (19% kg_w/kg_{dm}), the value of $MC_{avg,V}$ for the Reference Case in cool roof is 1.6% kg_w/kg_{dm} (41.6% RH) compared to 1.3% kg_w/kg_{dm} (36.8% RH) in black roof. During the first year, $MC_{avg,V}$ in the Fibreboard for the case of Fibreboard with HICM in cool roof reaches its lowest value of 2.8% kg_w/kg_{dm} (55.4% RH) after 293.1 day compared to only 0.5% kg_w/kg_{dm} (15.3% RH) after 196 day for the black roof (Fig-

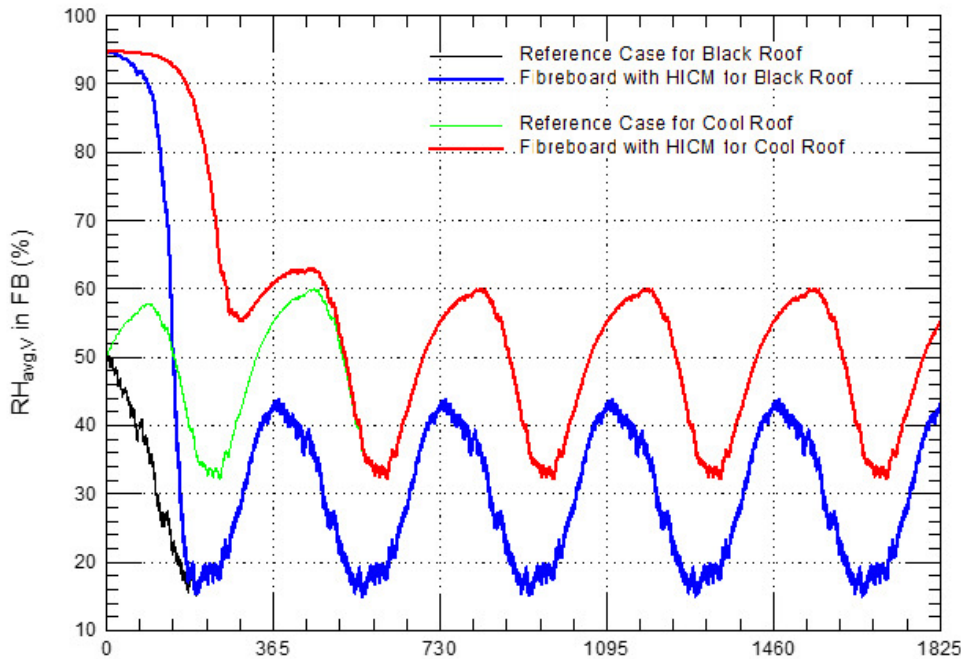


Figure 7. Volume-weighted average relative humidity ($RH_{avg,V}$) in the Fibreboard

ure 6). At the end of the first year, $MC_{avg,V}$ in the Fibreboard for the case of Fibreboard with HICM in cool roof is $3.5\% \text{ kg}_w/\text{kg}_{dm}$ (60.9% RH) compared to $1.7\% \text{ kg}_w/\text{kg}_{dm}$ (42.8% RH) for the black roof. Also, at the end of the first year, the value of $MC_{avg,V}$ for the Reference Case in cool roof is $2.8\% \text{ kg}_w/\text{kg}_{dm}$ (55.1% RH) compared to $1.7\% \text{ kg}_w/\text{kg}_{dm}$ (42.8% RH) for the black roof. Figure 6 shows that the difference between the moisture content in the Fibreboard for both Reference Case and Fibreboard with HICM has totally disappeared at time greater than 583 day in cool roof compared to 196 day in black roof. As such, times greater than these values (i.e., 196 day and 583 day, respectively, for black and cool roofs) have resulted in no effects of using different initial conditions on the moisture performance of black and cool roofs.

At 175.7 day, which is the time at which the value of $MC_{avg,V}$ reaches the threshold value of $19\% \text{ kg}_w/\text{kg}_{dm}$, Figure 8 shows that the value of $RH_{avg,A}$ on the Fibreboard top surface for the case of Fibreboard with HICM in cool roof is 85.3% ($12.5 \text{ kg}_w/\text{kg}_{dm}$) compared to 81.6% ($9.6\% \text{ kg}_w/\text{kg}_{dm}$ at 92.6 day) for black roof. Also, at 175.7 day, the value of $RH_{avg,A}$ on the Fibreboard bottom surface for the case of Fibreboard with HICM in cool roof is 92.2% ($24.1 \text{ kg}_w/\text{kg}_{dm}$) compared to 93.0% ($26.9\% \text{ kg}_w/\text{kg}_{dm}$ at 92.6 day) for black roof. However, for the Reference Case in cool roof at 175.7 day, the values of $RH_{avg,A}$ on the Fibreboard top surface and bottom surface, respectively, are 40.1% ($1.5\% \text{ kg}_w/\text{kg}_{dm}$) and 44.7% ($1.8\% \text{ kg}_w/\text{kg}_{dm}$) compared to 36.6% ($1.3\% \text{ kg}_w/\text{kg}_{dm}$) and 40.5% ($1.5\% \text{ kg}_w/\text{kg}_{dm}$) for the black roof. Finally, the moisture content or relative humidity on the Fibreboard top and bottom surfaces for the cool roof are identical for both the Reference Case and Fibreboard with HICM at time greater than 583 day compared to a time greater than 196 day for the black roof (Figure 7). Simi-

lar to many previous studies,^{18,21-24,37,46,48} the results provided above have clearly showed that cool roofs always run at higher moisture content in relation with black roofs.

Mould growth is one of the first signs of biological deterioration caused due to excess moisture in construction materials. Thus, mould formation can be used as one of the criteria for assessing the performance of building components/assemblies. In addition, mould is a sign of high moisture content and it represents a risk for other moisture-caused problems such as material deterioration. On the other hand, mould can affect the appearance of the surfaces and also can severely affect the indoor air quality when the mould growth is in contact with indoor air and/or with the leakage air flowing through the building assemblies into the room space called “air intrusion” (e.g., see^{27, 30} for more details). The level of mould index (M) of range 1 to 6⁵⁵⁻⁵⁷ is used in this study, where: (a) $M = 0$ represents no mould growth, (b) $M = 1$ represents initial stages of local mould growth with small amounts of mould on surface (detected by microscope), (c) $M = 2$ represents several local mould growth colonies on surface (detected by microscope), (d) $M = 3$ represents visual findings of mould on surface with < 10% coverage, (e) $M = 4$ represents visual findings of mould on surface with 10%–50% coverage, (f) $M = 5$ represents visual plenty of growth on surface with > 50% coverage, and finally (g) $M = 6$ visual heavy and tight growth with coverage about 100%.⁵⁷

The simulation results of both temperature and relative humidity are the key parameters that are needed for determining whether mould growth occurred. As provided in,⁵⁵⁻⁵⁷ for a relative humidity in a material layer less than critical relative humidity (RH_{crit}), which is a function of temperature, no mould growth occurs (i.e., $M = 0$). The expression for the RH_{crit} is given as⁵⁷:

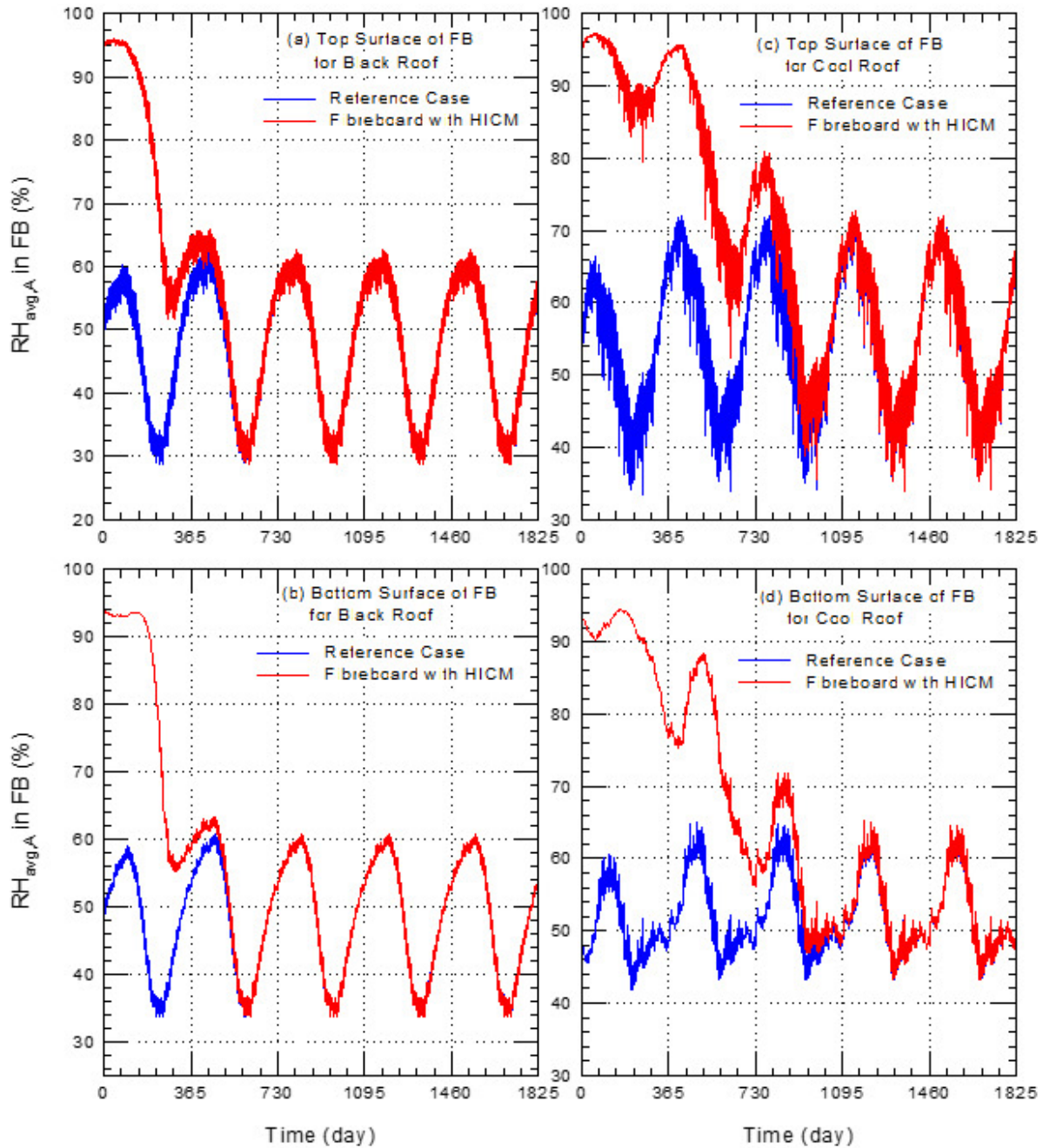


Figure 8. Area-weighted average RH on the Fibreboard top and bottom surfaces

$$RH_{Crit} = \begin{cases} -0.00267 T^3 + 0.16 T^2 - 3.13 T, & \text{when } T \leq 20 \\ RH_{min}, & \text{when } T > 20 \end{cases} \quad (4)$$

where RH_{Crit} and T in Eq. (4) are in % and °C, respectively. Also, RH_{min} in Eq. (4) equal 80% for very sensitive and sensitive mould classes, and 85% for medium resistant and resistant mould classes. As per the expression given in Eq. (4), RH_{Crit} decreases with increasing the temperature and reaches its lowest value (i.e., RH_{min}) at 20 °C. For a given relative humidity value that is greater than RH_{crit} , the mould index increases with increasing the temperature.⁵⁵⁻⁵⁷ For each material layer in the roofing system shown in Figure 1, the area- and volume-weighted average for both temperature and relative humidity obtained from the simulation results (see Eq. (2)) were used to determine

the mould index. In all simulations conducted in this study, the relative humidity values in the polyisocyanurate board were well below the critical relative humidity. As such, no mould growth occurs in the polyisocyanurate board. For the Reference Case in the roofing system, the relative humidity values in the Fibreboard for the black roof and the cool roof (Figure 7) were also well below the critical relative humidity, resulting in no mould growth occurred in the Fibreboard.

For the case of Fibreboard with HICM in black and cool roofs, the obtained results for the mould index are provided in Figure 9a for the whole Fibreboard, Figure 9b for the Fibreboard top surface, and Figure 9c for the Fibreboard bottom surface. For black roof, Figure 9a shows that the mould

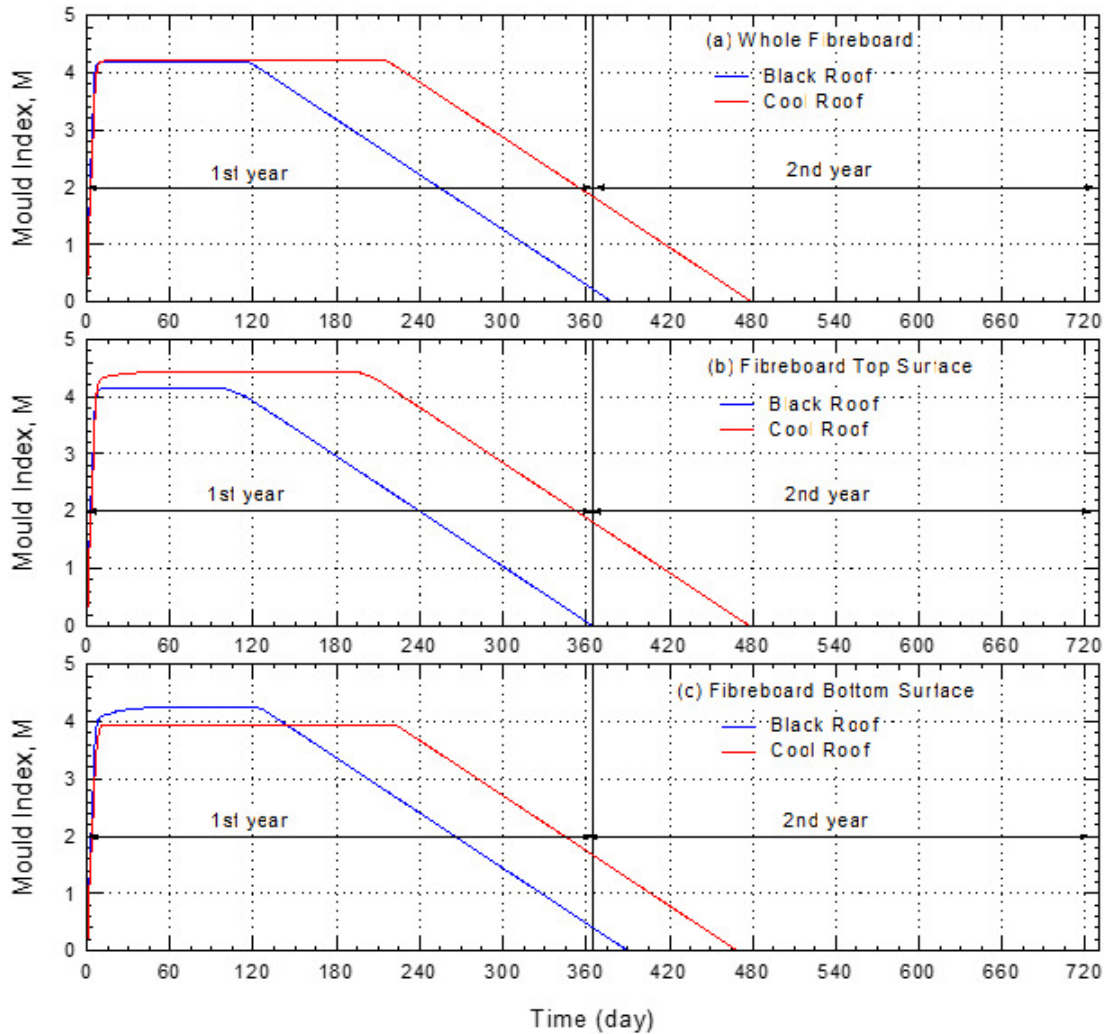


Figure 9. Mould index in the Fibreboard for the case of Fibreboard with HICM

index in the whole Fibreboard increases with time reaching its highest value of 4.18 at 8.5 day, and then it remains constant until 117 day. At time greater than 117 day, the mould index decreases with time reaching its lowest value ($M = 0$) at 378.8 day. Similarly, the mould index in the whole Fibreboard of the cool roof increases with time until it reaches its highest value of 4.20 at 12.9 day, and then it remains constant until $t = 217$ day; whereas at time greater than 217 day, the mould index decreases with time and reaches its lowest value of 0.0 at 479.3 day (Figure 9a). On the Fibreboard top surfaces, Figure 9b shows that the highest mold indexes for black roof and cool roof, respectively, are 4.14 and 4.46; whereas the mould has totally disappeared at 364.8 day and 478.1 day. Finally, Figure 9c shows that the highest mould indexes on the Fibreboard bottom surfaces for black roof and cool roof, respectively, are 4.24 and 3.94; whereas the mould has totally disappeared at 390.2 day and 469.3 day. Lastly, future studies are recommended to investigate the practical consequences related to the findings from this study such as material deteriorations, maintenance requirements, cost-effective retrofitting strategies for preventing mould to grow, etc.

THERMAL PERFORMANCE

As indicated earlier, the present model solves the HAM equations for the roofing systems considered in this study when they are subjected to natural weather conditions and the indoor conditions provided by Eq. (1). For the roofing system shown in Figure 1, results related to thermal gradient and temperature distributions as well as air velocity distributions in the enclosed-airspace between the steel deck and the vapour barrier are provided elsewhere.^{18,51} Using Eq. (2), the hourly area-weighted average temperature on the roof exterior surface ($T_{ext,s}$) are provided in Figure 10. In this study, α_s for the exterior surface of the black roof and cool roof are 12% and 80%, respectively.^{18,23} The simulation results during the year in which the effect of using various initial conditions on the hygrothermal performance (i.e., thermal performance and moisture performance) has totally disappeared are used to report the thermal performance of the black and cool roofs. This year is the second year for the black roof and the third year for cool roof. During the nighttime, Figure 10 shows that the exterior surface temperatures of the black roof are the same as those for the cool roof. For both black and cool roofs, the lowest exterior

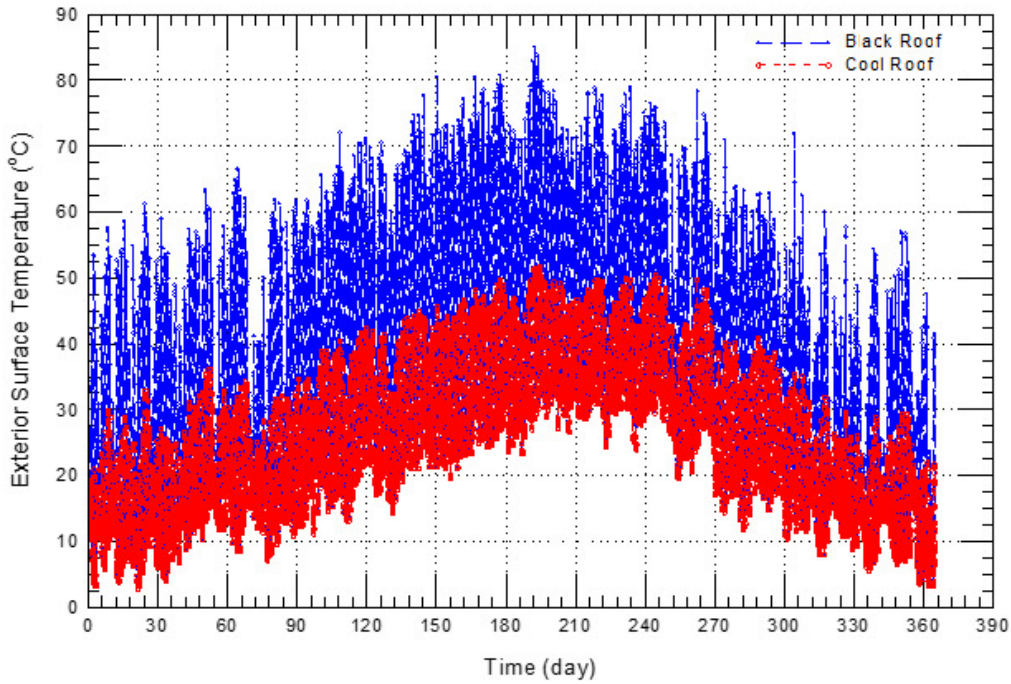


Figure 10. Comparison of hourly exterior surface temperatures for black and cool roofs

surface temperature is 2.9 °C (occurred in January at $t = 510$ h). During the daytime, however, due to lower α_s for black roof ($\alpha_s = 12\%$) than that for cool roof ($\alpha_s = 80\%$), more solar energy is absorbed in the black roof than that in the cool roof. This has resulted in that the exterior surface temperatures of the black roof during the daytime is greater than those for the cool roof as shown [Figure 10](#). The highest exterior surface temperature for the black roof is 85.1 °C (occurred in July at $t = 4931$ h), which is higher than that for cool roof by 33.6 °C ($T_{\text{ext},s} = 51.5$ °C).

[Figure 11](#) shows comparisons of the monthly average temperature for the exterior surfaces of the black and cool roofs. For black roof and cool roof, respectively, the highest monthly average temperatures occurs in July, which are 46.9 °C and 37.8 °C; whereas the lowest monthly average temperatures occurs in December, which are 18.7 °C and 12.6 °C. During the whole year, the highest differences between the monthly average temperatures of the exterior surfaces of the black and cool roofs is 10.2 °C (occurred in June). Additionally, the lowest differences between the monthly average temperatures for black and cool roofs is 5.8 °C (occurred in January).

As provided in Eq. (3), the simulation results for the heat fluxes on the indoor surfaces of the black and cool roofs were used to determine the heating loads and the cooling loads. The procedure that was used for determining these loads is provided in ^{18,37}. The results provided in [Figure 12](#) and [Figure 13](#) represent the contributions to the monthly cooling and heating loads per square meter of the conditioned area of the roof shown in [Figure 1](#). For the black roof and cool roof, respectively, [Figure 12](#) and [Figure 13](#) show the monthly cooling and heating loads. These figures show that the monthly cooling loads for the black roof are much greater than that for cool roof. For example, the monthly

cooling load in July with the black roof (254.9 W-day/m²) is 1.8 times the monthly cooling load with the cool roof (142.1 W-day/m²). Furthermore, the total yearly cooling load with black roof (1682.0 W-day/m²) is 2.4 times the total yearly cooling load with the cool roof (701.7 W-day/m²). Conversely, the total yearly heating load with the cool roof (469.0 W-day/m²) is 22% greater than that with the black roof (384.7 W-day/m²). Finally, the total yearly cooling and heating loads for the black roof (2066.7 W-day/m²) is 77% greater than that with the cool roof (1170.6 W-day/m²).

It is important to point out that this study focusses only on the energy and moisture performance of one assembly/component of the building envelope (black and cool roofs). Assessing the indoor air quality and the corresponding indoor thermal comfort, however, requires assessing the performance of the whole building rather than the performance of only one building assembly (e.g., see⁵⁸⁻⁶⁰ for more details).

CONCLUSIONS

In this study, an advanced and validated numerical model was used to assess the long-term performance of black and cool Modified-Bitumen (MOD-BIT) roofs, subjected to Phoenix climate. The simulations were conducted to: (a) assess the moisture performance of cool and black roofs in case of using material layer (Fibreboard in this study) with high initial construction moisture content, called “Fibreboard with HICM”, (b) identify the time needed so that the moisture content would reach acceptable value, (c) determine whether mould growth occurs in the roofs, and (d) determine the energy savings as a result of using cool roof instead of black roof. The results showed that for the case of Fibreboard with HICM, the moisture content in the Fibre-

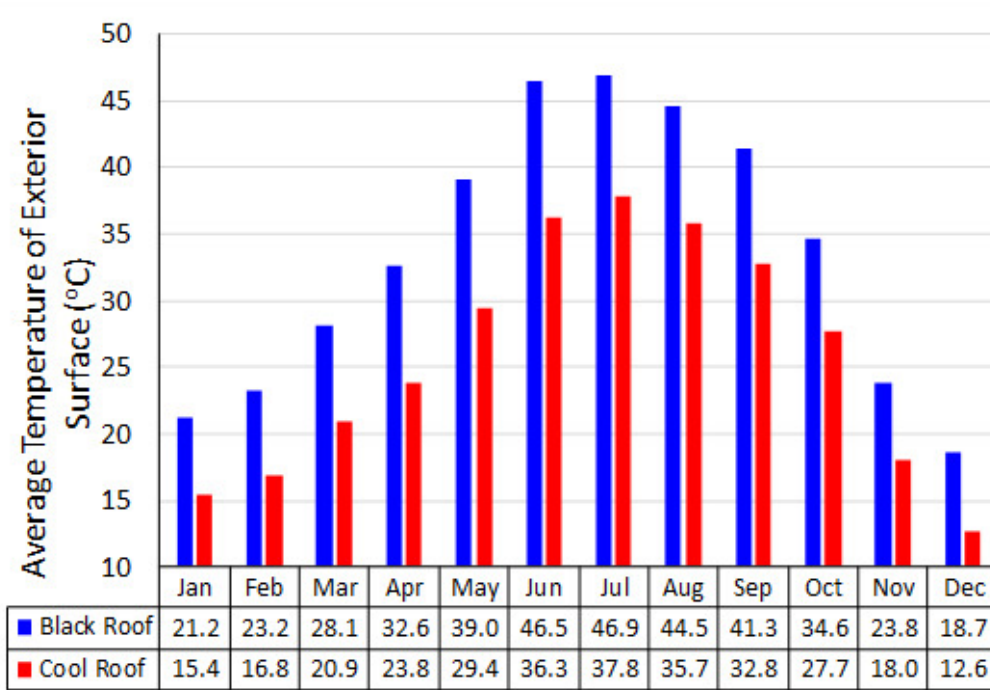


Figure 11. Comparisons of monthly average exterior surface temperatures for black and cool roofs

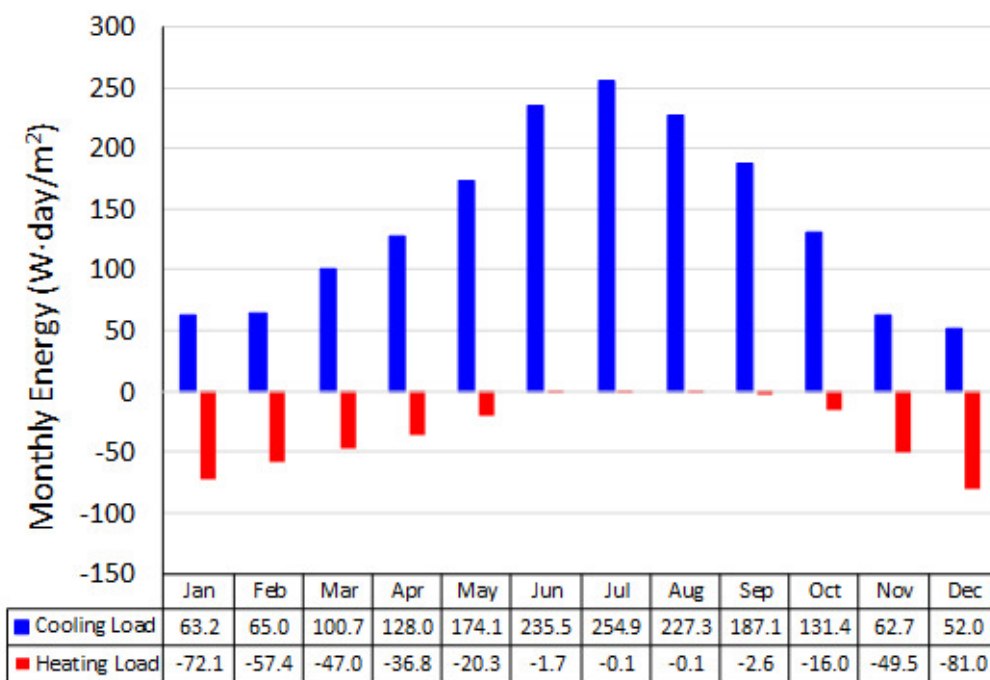


Figure 12. Comparisons of the monthly cooling and heating loads for black roof

board for the black roof and cool roof, respectively, has decreased from the initial value to the permissible value after 92.6 day and 175.7 day. The effect of using different initial conditions in both Reference Case and Fibreboard with HICM on the performance has totally disappeared after 196 day for black roof and 583 day for cool roof. For the case of Fibreboard with HICM only, mould growth occurred in the Fibreboard of both black and cool roofs. In addition, the mould has totally disappeared in the whole Fibreboard

of black roof and cool roof after 378.8 day and 479.3 day, respectively. For the thermal performance, the total yearly cooling load with the black roof was 2.4 times that with cool roof. Conversely, the total yearly heating load with the cool roof was only 22% higher than that with the black roof.

Submitted: January 27, 2024 AST, Accepted: June 03, 2024 AST

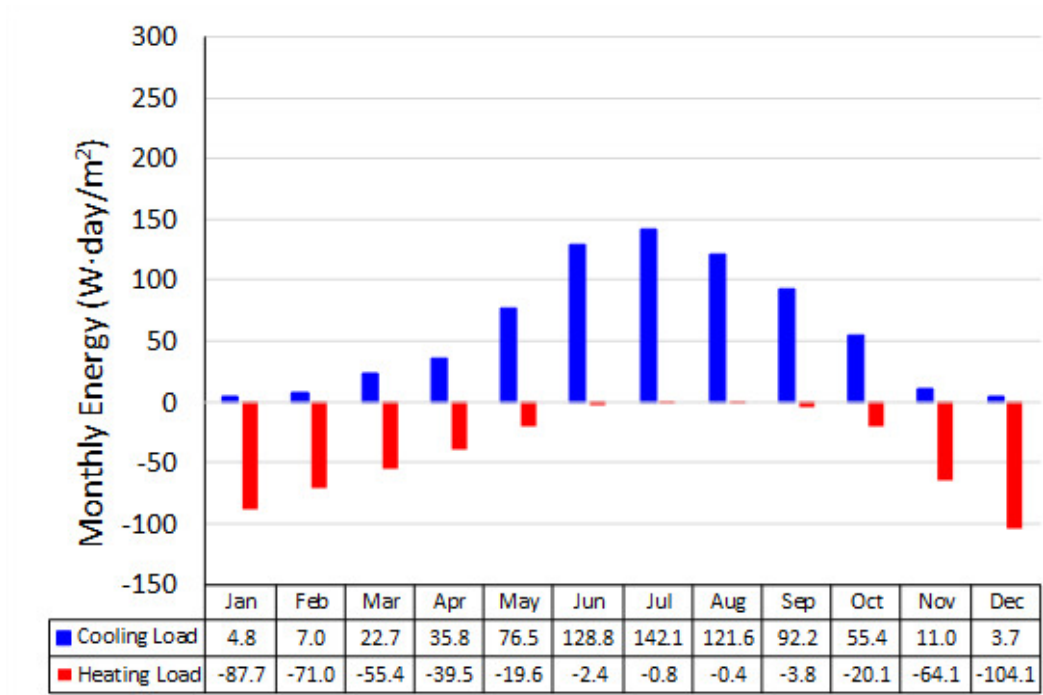


Figure 13. Comparisons of the monthly cooling and heating loads for cool roof



This is an open-access article distributed under the terms of the Creative Commons Attribution 4.0 International License (CCBY-4.0). View this license's legal deed at <http://creativecommons.org/licenses/by/4.0> and legal code at <http://creativecommons.org/licenses/by/4.0/legalcode> for more information.

REFERENCES

1. Solecki WD, Rosenzweig C, Parshall L, et al. Mitigation of the heat island effect in urban New Jersey. *Environmental Hazards*. 2005;6(1):39-49. [doi:10.1016/j.hazards.2004.12.002](https://doi.org/10.1016/j.hazards.2004.12.002)
2. Al-Homoud MS. Performance characteristics and practical applications of common building thermal insulation materials. *Building and Environment*. 2005;40:353-366. [doi:10.1016/j.buildenv.2004.05.013](https://doi.org/10.1016/j.buildenv.2004.05.013)
3. Tariku F, Shang Y, Molleti S. Thermal performance of flat roof insulation materials: A review of temperature, moisture and aging effects. *Journal of Building Engineering*. 2023;76(3):107142. [doi:10.1016/j.jobbe.2023.107142](https://doi.org/10.1016/j.jobbe.2023.107142)
4. Yousefi Y, Tariku F. Thermal conductivity and specific heat capacity of insulation materials at different mean temperatures. *Journal of Physics: Conference Series*. 2021;2069:012090. [doi:10.1088/1742-6596/2069/1/012090](https://doi.org/10.1088/1742-6596/2069/1/012090)
5. Levinson R, Akbari H, Berdahl P, Wood K, Skilton W, Petersheim J. A novel technique for the production of cool colored concrete tile and asphalt shingle roofing products. *Solar Energy Materials and Solar Cells*. 2010;94(6):946-954. [doi:10.1016/j.solmat.2009.12.012](https://doi.org/10.1016/j.solmat.2009.12.012)
6. Oleson KW, Bonan GB, Feddema J. Effects of white roofs on urban temperature in a global climate model. *Geophysical Research Letters*. 2010;37(3):art.no.L03701. [doi:10.1029/2009GL042194](https://doi.org/10.1029/2009GL042194)
7. Kaood A, ElDegwy A, Aboulmagd A. Hydrothermal and entropy generation performance of convergent tubes with various dimple shapes. *International Journal of Thermal Sciences*. 2024;197:108842. [doi:10.1016/j.ijthermalsci.2023.108842](https://doi.org/10.1016/j.ijthermalsci.2023.108842)
8. Wei H, Moria H, Nisar KS, et al. Effect of volume fraction and size of Al₂O₃ nanoparticles in thermal, frictional and economic performance of circumferential corrugated helical tube. *Case Studies in Thermal Engineering*. 2021;25:100948. [doi:10.1016/j.csite.2021.100948](https://doi.org/10.1016/j.csite.2021.100948)
9. Kaood A, Aboulmagd A, Othman H, ElDegwy A. Numerical investigation of the thermal-hydraulic characteristics of turbulent flow in conical tubes with dimples. *Case Studies in Thermal Engineering*. 2022;36:102166. [doi:10.1016/j.csite.2022.102166](https://doi.org/10.1016/j.csite.2022.102166)
10. McHugh B, Petrick R. Chicago's green and garden roofing codes and technology. In: *Proceedings of the 2011 International Roofing Symposium*. ; 2011.
11. Durhman A, Collins M, McGillis WR. Utilizing green technology and research to assess green roofing benefits. In: *Proceedings of the 2011 International Roofing Symposium*. ; 2011.
12. Tariku F, Hagos S. Performance of green roof installed on highly insulated roof deck and the plants' effect: An experimental study. *Building and Environment*. 2022;221:109337. [doi:10.1016/j.buildenv.2022.109337](https://doi.org/10.1016/j.buildenv.2022.109337)
13. Bentz SP. Decision-making process for green options in reroofing. In: *Proceedings of the 2011 International Roofing Symposium*. ; 2011.
14. Akbari H, Konopacki S, Pomerantz M. Cooling energy savings potential of reflective roofs for residential and commercial buildings in the United States. *Energy*. 1999;24(5):391-407. [doi:10.1016/S0360-5442\(98\)00105-4](https://doi.org/10.1016/S0360-5442(98)00105-4)
15. Akbari H, Konopacki S, Parker D. Updates on revision to ASHRAE standard 90.2: Including roof reflectivity for residential buildings. In: *Proceedings ACEEE Summer Study on Energy Efficiency in Buildings*. Vol 1. ; 2000:11-111.
16. Ray S, Glicksman L. Potential energy savings of various roof technologies. In: *Eleventh International Conference on Thermal Performance of the Exterior Envelopes of Whole Buildings XI*. ; 2010.
17. Brehob E, Desjarlais A, Atchley J. Effectiveness of cool roof coatings with ceramic particles. Presented at: 2011 International Roofing Symposium; September 7–9, 2011; Washington D.C., USA.
18. Saber HH, Swinton MC, Kalinge P, Paroli RM. Long-term hygrothermal performance of white and black roofs in North American climates. *Building and Environment*. 2012;50(18):141-154. [doi:10.1016/j.buildenv.2011.10.022](https://doi.org/10.1016/j.buildenv.2011.10.022)
19. Urban B, Roth K. *Guidelines for Selecting Cool Roofs*. U.S. Department of Energy, Energy Efficiency and Renewable Energy, Building Technologies Program; 2010.
20. Hutchinson T. Cool roofing challenging what's cool. Eco-structure. 2009. Accessed December 2023. <http://www.eco-structure.com/cool-roofing/challenging-whats-cool.aspx>
21. Desjarlais AO. Self-drying roofs: what?! no dripping! In: *Proceedings of Thermal Performance of Exterior Envelopes of Buildings VI*. ; 1995:763-773.

22. Ennis M, Kehrer M. The effects of roof membrane color on moisture accumulation in low-slope commercial roof systems. In: *Proceedings of the 2011 International Roofing Symposium.* ; 2011.
23. Bludau C, Zirkelbach D, Kuenzel HM. Condensation problems in cool roofs. *Interface, the Journal of RCI.* 2009;XXVII(7):11-16.
24. Bludau C, Künzel HM, Zirkelbach D. Hygrothermal performance of flat roofs with construction moisture. Presented at: Eleventh International Conference on Thermal Performance of the Exterior Envelopes of Whole Buildings XI; December 4–9, 2010; Clearwater, FL, USA.
25. *National Building Code of Canada (2010) Issued by Canadian Commission on Building and Fire Codes.* Vol 2, Division B, Appendix C. National Research Council of Canada
26. Saber HH, Maref W, Lacasse MA, Swinton MC, Kumaran MK. Benchmarking of hygrothermal model against measurements of drying of full-scale wall assemblies. In: *2010 International Conference on Building Envelope Systems and Technologies, ICBEST 2010.* ; 2010:369-377.
27. Saber HH, Maref W, Elmahdy AH, Swinton MC, Glazer R. 3D heat and air transport model for predicting the thermal resistances of insulated wall assemblies. *Int J of Building Performance Simulation.* 2012;5(2):75-91. [doi:10.1080/19401493.2010.532568](https://doi.org/10.1080/19401493.2010.532568)
28. Saber HH, Maref W, Swinton MC, St-Onge C. Thermal analysis of above-grade wall assembly with low emissivity materials and furred airspace. *Building and Environment.* 2011;46(7):1403-1414. [doi:10.1016/j.buildenv.2011.01.009](https://doi.org/10.1016/j.buildenv.2011.01.009)
29. Saber HH, Yarbrough DW. Advanced modeling of enclosed-airspaces to determine thermal resistance for building applications. *Energies.* 2021;14(22):7772.
30. Saber HH, Yarbrough DW. Assessing the effect of air intrusion on reflective insulations performance with horizontal heat flow. *Buildings.* 2023;13(10):2461.
31. Saber HH, Maref W, Sherrer G, Swinton MC. Numerical modelling and experimental investigations of thermal performance of reflective insulations. *J of Building Physics.* 2012;36(2):163-177. [doi:10.1177/1744259112444021](https://doi.org/10.1177/1744259112444021)
32. Saber HH. Investigation of thermal performance of reflective insulations for different applications. *Building and Environment.* 2012;52:32-44. [doi:10.1016/j.buildenv.2011.12.010](https://doi.org/10.1016/j.buildenv.2011.12.010)
33. Saber HH, Maref W, Armstrong M, Swinton MC, Rousseau MZ, Gnanamurugan G. Benchmarking 3D thermal model against field measurement on the thermal response of an insulating concrete form (ICF) wall in cold climate. In: *Building XI Conference.* ; 2010.
34. Saber HH, Maref W, Gnanamurugan G, Nicholls M. Model Benchmarking for Field Energy Retrofit towards Highly Insulated Residential Wood-Frame Construction Using VIPs. In: *11th International Vacuum Insulation Symposium (IVIS2013).* ; 2013.
35. Saber HH, Maref W, Gnanamurugan G, Nicholls M. Can VIP Be an Alternative Solution for Energy Retrofit for Enhancing the Thermal Performance of Wood-Frame Walls? In: *The Twelfth International Conference on Thermal Performance of the Exterior Envelopes of Whole Buildings (Buildings XII Conference).* ; 2013. [doi:10.1177/1744259113505748](https://doi.org/10.1177/1744259113505748)
36. Saber HH, Maref W, Gnanamurugan G, Nicholls M. Energy Retrofit Using Vacuum Insulation Panels: An Alternative Solution for Enhancing the Thermal Performance of Wood-Frame Walls. *Journal of Building Physics.* 2015;39(1):35-68. [doi:10.1177/1744259113505748](https://doi.org/10.1177/1744259113505748)
37. Saber HH, Maref W, Hajiah AE. Hygrothermal performance of cool roofs subjected to Saudi climates. *J of Frontiers in Energy Research.* 2019;7(39):1-24. [doi:10.3389/fenrg.2019.00039](https://doi.org/10.3389/fenrg.2019.00039)
38. Saber HH, Maref W. Energy performance of cool roofs followed by development of practical design tool. *J of Frontiers in Energy Research.* 2019;7(122):1-22. [doi:10.3389/fenrg.2019.00122](https://doi.org/10.3389/fenrg.2019.00122)
39. ASTM C1363. Standard test method for thermal performance of building materials and envelope assemblies by means of a hot box apparatus. In: *Annual Book of ASTM Standards.* Vol 04.06. ; 2021:792-836.
40. ASTM C518. Standard test method for steady-state heat flux measurements and thermal transmission properties by means of the heat flow meter apparatus. In: Vol 04.06. ASTM-International; 2021:163-178.
41. Saber HH, Maref W, Sherrer G, Swinton MC. Numerical modeling and experimental investigations of thermal performance of reflective insulations. *J Build Phys.* 2012;36:163-177.
42. Saber HH. Investigation of thermal performance of reflective insulations for different applications. *Build Environ.* 2011;52:32-44.

43. Robinson HE, Powlitch (Powell) FJ. *The Thermal Insulating Value of Airspaces*. U.S. National Bureau of Standards; 1956.
44. Kumaran MK, Lackey J, Normandin N, Tariku F, van Reenen D. *A Thermal and Moisture Transport Property Database for Common Building and Insulating Materials*. Final Report from ASHRAE Research Project 1018-RP; 2004:1-229.
45. ASHRAE. Chapter 26, Table 3. In: *ASHRAE Handbook of Fundamental, Effective Thermal Resistance of Plane Air Spaces*. ; 2021:26.14-26.15.
46. Saber HH. Hygrothermal performance of cool roofs with reflective coating material subjected to hot, humid and dusty climate. *J of Building Physics*. 2022;45(4):457-481. [doi:10.1177/17442591211001408](https://doi.org/10.1177/17442591211001408)
47. Saber HH. Experimental characterization of reflective coating material for cool roofs in hot, humid and dusty climate. *Energy and Buildings*. Published online 2021:110993. [doi:10.1016/j.enbuild.2021.110993](https://doi.org/10.1016/j.enbuild.2021.110993)
48. Saber HH, Hajiah AE, Alshehri SA, Hussain HJ. Investigating the effect of dust accumulation on solar reflectivity of coating materials for cool roof applications. *Energies*. 2021;14(2):1-28. [doi:10.3390/en14020445](https://doi.org/10.3390/en14020445)
49. ASHRAE. Chapter 3 – Commercial and Public Buildings. In: *ASHRAE Handbook – Applications*. American Society of Heating, Refrigerating and Air-Conditioning Engineers, Inc.; 2003.
50. EN 15026 (2007) Hygrothermal performance of building components and building elements – assessment of moisture transfer by numerical simulation. European Committee for Standardization.
51. Saber HH, Swinton MC, Kalinger P, Paroli RM. Hygrothermal Simulations of Cool Reflective and Conventional Roofs. In: *Proceedings of the 2011 International Roofing Symposium*. ; 2011:1-28.
52. Hajiah AE, Saber HH. Long-Term Energy and Moisture Performance of Reflective and Non-Reflective Roofing Systems with and without Phase Change Materials under Kuwaiti Climates. In: Bumajdad A, Bouhamra W, Alsayegh O, Kamal H, Alhajraf S, eds. *Gulf Conference on Sustainable Built Environment*. Springer; 2020:453-482.
53. Saber HH, Hajiah AE, Maref M. Hygrothermal Performance of Cool Roofs Subjected to Hot and Humid Climates. In: *2019 Buildings XIV International Conference*. ; 2019:410-420.
54. Saber HH, Hajiah AE, Maref W. Impact of Reflective Roofs on the Overall Energy Savings of Whole Buildings. In: *12th Nordic Symposium on Building Physics (NSB 2020), Section of Energy Performance Simulation and Assessment*. Vol 172. ; 2020:1-13. [doi:10.1051/e3sconf/202017225008](https://doi.org/10.1051/e3sconf/202017225008)
55. Hukka A, Viitanen HA. A mathematical model of mould growth on wooden material. *Wood Science and Technology*. 1999;33(6):475-485. [doi:10.1007/s002260050131](https://doi.org/10.1007/s002260050131)
56. Viitanen HA, Ojanen T. Improved model to predict mould growth in building materials. In: *Proceedings of Thermal Performance of the Exterior Envelopes of Whole Buildings X*. ; 2007:8.
57. Ojanen T, Viitanen HA, Peuhkuri R, Lähdesmäki K, Vinha J, Salminen K. Mold growth modeling of building structures using sensitivity classes of materials. Presented at: 11th International Conference on Thermal Performance of the Exterior Envelopes of Whole Buildings XI; December 5, 2010; Clearwater, FL, USA.
58. Heibati S, Maref W, Saber HH. Assessing the Energy and Indoor Air Quality Performance for 3-Story Building Using Integrated Model, Part 1: The Need for Integration. *Energies*. 2019;12(4775):1-18. [doi:10.3390/en12244775](https://doi.org/10.3390/en12244775)
59. Heibati S, Maref W, Saber HH. Assessing the Energy, Indoor Air Quality and Moisture Performance for a Three-Story Building Using an Integrated Model, Part Two: Integrating the Indoor Air Quality, Moisture and Thermal Comfort. *Energies*. 2021;14:4915. [doi:10.3390/en14164915](https://doi.org/10.3390/en14164915)
60. Heibati S, Maref W, Saber HH. Assessing the Energy, Indoor Air Quality, and Moisture Performance for a Three-Story Building Using an Integrated Model, Part Three: Development of Integrated Model and Applications. *Energies*. 2021;14:5648.